Development 139, 2050-2060 (2012) doi:10.1242/dev.078360

Laminin is required to orient epithelial polarity in the *C. elegans* pharynx

Jeffrey P. Rasmussen[1,2,3], Sowmya Somashekar Reddy[1,2] and James R. Priess[1,2,4,*]

SUMMARY

The development of many animal organs involves a mesenchymal to epithelial transition, in which cells develop and coordinate polarity through largely unknown mechanisms. The *C. elegans* pharynx, which is an epithelial tube in which cells polarize around a central lumen, provides a simple system with which to understand the coordination of epithelial polarity. We show that cell fate regulators cause pharyngeal precursor cells to group into a bilaterally symmetric, rectangular array of cells called the double plate. The double plate cells polarize with apical localization of the PAR-3 protein complex, then undergo apical constriction to form a cylindrical cyst. We show that laminin, but not other basement membrane components, orients the polarity of the double plate cells. Our results provide in vivo evidence that laminin has an early role in cell polarity that can be distinguished from its later role in basement membrane integrity.

KEY WORDS: Epithelial polarity, Laminin, Mesenchymal to epithelial transition, Morphogenesis, Tubulogenesis

INTRODUCTION

Cells exhibit multiple asymmetries during animal development in response to successive cues that create and change cell polarity. For example, the one-cell *C. elegans* embryo develops anterior-posterior polarity cued by the sperm-contributed centrosome, but blastomeres at the four-cell stage exhibit inner-outer polarity cued by cell contacts (reviewed by Nance and Zallen, 2011). Perhaps the most dramatic changes in cell polarity occur during tissue and organ morphogenesis, when large groups of mesenchymal cells coordinately polarize to form epithelial sheets or tubes, an event termed mesenchymal to epithelial transition (MET) (reviewed by Chaffer et al., 2007).

Studies using cultured cells have long suggested that extracellular matrix components such as laminin and collagen might function as polarity cues for developing epithelia (Ekblom, 1989). Laminin is a secreted heterotrimeric protein composed of α, β and γ subunits. Cells use laminin receptors, such as integrins and dystroglycans, to bind and polymerize laminin at the cell surface. Laminin is an integral basement membrane component and can act as a scaffold for the assembly of other components (reviewed by Yurchenco, 2011). Mutations in laminin can cause widespread developmental abnormalities in mice and humans, and the expression of certain laminin heterotrimers is causally related to the development of some aggressive, malignant epithelial cancers in humans (reviewed by Marinkovich, 2007; Miner and Yurchenco, 2004). Evidence that laminin might function as a polarizing cue during MET has come primarily from work on cultured mammalian kidney cells. After several days in three-dimensional culture, Madin-Darby canine kidney (MDCK) cells form epithelial cysts that differentiate apical surfaces facing an internal lumen. MDCK cysts can develop inverted polarity when grown without basement membrane-containing substrate or after expression of a dominant-negative Rac1 (O'Brien et al., 2001; Wang et al., 1990). Addition of high levels of exogenous laminin can rescue this inverted polarity, suggesting that laminin can orient MDCK polarity (O'Brien et al., 2001). In other studies, antibodies against laminin α1 were shown to block epithelial polarization in kidney organ culture (Klein et al., 1988). Thus, laminin might function to either initiate or orient polarity in the cultured cells.

The analysis of laminin function in mice and humans is complicated by the presence of at least 16 laminin heterotrimers (Aumailley et al., 2005) and by the severe defects associated with mutations in even single laminin subunits (Miner et al., 1998; Miner and Yurchenco, 2004; Ryan et al., 1999; Smyth et al., 1999). In *C. elegans*, only two laminin heterotrimers are assembled, composed of either of the two laminin α subunits LAM-3 or EPI-1, and single laminin β and γ subunits called LAM-1 and LAM-2, respectively (Huang et al., 2003). *lam-3* and *epi-1* mutants have complex terminal phenotypes, including ruptured tissues, ectopic cell adhesions and abnormally positioned adherens junctions (Huang et al., 2003). Developmental studies have not resolved whether these abnormalities result from primary defects in cell polarity or from more general requirements for basement membranes in tissue integrity and support.

In the present study, we analyze how embryonic cells that form the *C. elegans* pharynx acquire and coordinate their polarity and how laminin affects these events. The pharynx is an elongated epithelial tube that contains myoepithelial cells, epithelial support cells, glands and neurons (Albertson and Thomson, 1976). The pharynx develops from pharyngeal precursor cells (PPCs) that cluster together to form a primordium in the interior of the embryo. Through unknown mechanisms, the primordium undergoes a MET to transform into a short, cylindrical epithelial cyst; the cyst elongates and narrows during subsequent development to form the pharyngeal tube (Leung et al., 1999; Portereiko and Mango, 2001). The cyst represents the architectural foundation for later pharyngeal differentiation, prefiguring the basic symmetry and patterning of the mature pharynx. Although some pharyngeal cells migrate and/or develop elaborate shapes (Mörck et al., 2003; Raharjo et al., 2011; Rasmussen et al., 2008), many of the cells in the mature

[1]Fred Hutchinson Cancer Research Center, Seattle, WA 98109, USA. [2]Howard Hughes Medical Institute, Seattle, WA 98019, USA. [3]Molecular and Cellular Biology Program, University of Washington, Seattle, WA 98195, USA. [4]Department of Biology, University of Washington, Seattle, WA 98195, USA.

*Author for correspondence (jpriess@fhcrc.org)

Accepted 19 March 2012

pharynx retain their basic shapes and positions in the cyst. The PAR-3 complex (PAR-3, PAR-6 and PKC-3) is associated with early stages of epithelial polarity in many systems (Nance and Zallen, 2011) and localizes to the apical surfaces of cyst stage PPCs (Bossinger et al., 2001; Leung et al., 1999; McMahon et al., 2001). PAR-3 function is required for the subsequent apical localization of several proteins in pharyngeal cells, including components of adherens junctions (Achilleos et al., 2010). However, the molecular cues that localize the PAR-3 complex to the apical surfaces of PPCs have not been identified.

We show that development of the pharyngeal cyst is preceded by a distinct morphogenetic intermediate that we call the double plate. PPC polarization and PAR localization begin in the double plate, which transforms into a cyst by apical constriction. We show that laminin provides a crucial cue that orients apical localization of the PAR-3 complex in the double plate PPCs. Surprisingly, laminin function does not appear necessary to orient the apical localization of the PAR-3 complex in the *C. elegans* intestine, a second type of epithelial tube. Thus, different epithelial organs appear to utilize at least partially distinct polarity cues, and pharyngeal development provides a model for laminin-based signaling in epithelial polarity.

MATERIALS AND METHODS

Nematodes

C. elegans were cultured as described (Brenner, 1974). Mutant alleles used (details available at http://www.wormbase.org): LG I, *lam-3(n2561)* (Huang et al., 2003); LG II, *unc-52(st549)* (Williams and Waterston, 1994); LG III, *unc-119(ed3)* (Maduro and Pilgrim, 1995), *wrm-1(ne1982)* (Nakamura et al., 2005), *unc-36(e251) emb-9(g23cg46)* (Gupta et al., 1997), *pat-3(st564)* (Williams and Waterston, 1994); LG IV, *lam-1(ok3139,ok3221), epi-1(rh199)* (Zhu et al., 1999); LG V, *fog-2(q71) pha-4(q490)* (Mango et al., 1994). Transgenes used: *stIs10088* [*hlh-1(3.3kb)*::HIS-24::mCherry] (Murray et al., 2008), *pxIs6* [*pha-4*::GFP::HIS-11] (Portereiko and Mango, 2001), *wgIs37* [PHA-4::TY1::EGFP::3xFLAG] (Zhong et al., 2010), *zuIs45* [*nmy-2*::NMY-2::GFP] (Nance et al., 2003), *xnIs3* [*par-6*::PAR-6::GFP] (Totong et al., 2007), *pie-1*::mCherry::PAR-6 (Schonegg et al., 2007), *urEx131* [*lam-1*::LAM-1::GFP] (Kao et al., 2006), *qyIs43* [PAT-3::GFP; *ina-1*(genomic)] (Hagedorn et al., 2009), *ltIs44* [*pie-1*::mCherry::PH(PLC1δ1)] (Kachur et al., 2008), *zuEx276, zuIs270* [*pha-4*::GFP::dMoesin-ABD], *zuEx254* [*lin-12*^{pm8}::mCherry::CAAX; *lin-12*^{pm8}::GFP::HIS-11] and *zuEx288* [*lam-1(+);* SUR-5::GFP]. RNAi against *mex-1* and *pat-3* was performed using previously described double-stranded (ds) RNA feeding strains (Kamath et al., 2003; Tenlen et al., 2006). Developmental staging of embryos was performed as described (Sulston et al., 1983).

Transgene construction

To create pSSR18 [*pha-4*::GFP::dMoesin-ABD], the dMoesin-ABD fragment from pJWZ6 (Ziel et al., 2009) was PCR amplified, fused to GFP and cloned into the *Avr*II and *Apa*I sites of pJIM20-*pha-4* (Murray et al., 2008). *zuEx276* was created by injection of pSSR18 at 20 ng/μl and pJN254 at 100 ng/μl (Nance et al., 2003) into *unc-119(ed3)* worms, and integrated by gamma irradiation to create *zuIs270*. Construction of *zuEx254* will be described elsewhere.

Imaging

Embryos were mounted for longitudinal optical sectioning as described (Sulston et al., 1983). For transverse sectioning with confocal microscopy, ~4 cm^2 pieces of 35 micron Nitex mesh (Dynamic Aqua-Supply, Surrey, Canada) were treated with 1% osmium tetroxide (Sigma) overnight and then washed extensively; this treatment reduces Nitex autofluorescence. Embryos were pipetted in a small volume of liquid onto a piece of the Nitex filter on top of a 3% agarose pad. The embryos/filter were covered with a coverslip and sealed with petroleum jelly. Time-lapse movies were acquired with a spinning disk confocal system (Yokogawa CSU-10) on a Nikon TE-2000 inverted microscope equipped with a Hamamatsu C9100 camera, running Volocity 5.3.3 (Improvision, Lexington, MA, USA). 60× and 100× oil-immersion objectives (Nikon) were used for longitudinal optical sectioning, and a 60× water-immersion objective (Nikon) was used for transverse sectioning. Image stacks were analyzed and adjusted for brightness and contrast using ImageJ (http://rsbweb.nih.gov/ij/) or Adobe Photoshop. Brightness and contrast were adjusted for each time point separately. Quantification of midplane enrichment of NMY-2 and PAR-6 was performed by analyzing maximum intensity projections of longitudinal views of embryos co-expressing NMY-2::GFP and mCherry::PAR-6. The integrated intensities in two 5×12 μm regions (PPC midplane and PPC lateral) were corrected for camera noise, and then normalized to the initial time point. The midplane enrichment at time i was calculated as: $(PPC_{mid;\ t=i}/PPC_{lateral;\ t=i})/(PPC_{mid;\ t=0}/PPC_{lateral;\ t=0})$. Confidence intervals were calculated using Microsoft Excel.

Immunofluorescence

Fixation and staining of embryos were performed as described (Leung et al., 1999). The following primary antibodies and antisera were used: rabbit anti-GFP (ab6556, Abcam), anti-UNC-52 (Mullen et al., 1999), anti-LET-2 (Graham et al., 1997), rat anti-NMY-1 (Piekny et al., 2003), mouse anti-PAR-3 (Nance et al., 2003), MH25 (Francis and Waterston, 1985), mAbGJ1 (anti-LAM-3), mAbGJ2 (pan-laminin) (Rasmussen et al., 2008), IFA (Pruss et al., 1981) and mAbPL1 (G. Hermann and J.R.P., unpublished). For quantification of centrosome orientation, image stacks were acquired of PHA-4::GFP-expressing embryos immunostained with GFP and IFA antibodies (a marker of centrosomes) (Leung et al., 1999).

Characterization of *lam-1* mutants

lam-1 deletion alleles *ok3139* and *ok3221* were generated by the international *C. elegans* Gene Knockout Consortium. *ok3139* was outcrossed five times and maintained over the GFP-marked balancer *nT1[qIs51]* or the visible marker *unc-5(e53)*. Alleles *ok3139* and *ok3221* were sequenced and both found to cause frameshifts N-terminal to the coiled-coil domains required for assembly of the laminin subunits (supplementary material Fig. S2A) (Miner and Yurchenco, 2004); thus, these mutations are predicted to eliminate heterotrimer secretion. Embryos homozygous for either allele are embryonic lethal, and *lam-1(ok3221)* embryos show a multi-lumen phenotype similar to that described here for *lam-1(ok3139)* (data not shown). The *ok3139* mutation was fully rescued by the fosmid WRM0633dC11, which contains the wild-type *lam-1* locus. For mosaic analysis, *lam-1(ok3139)/nT1[qIs51]* adults were injected with WRM0633dC11 at 10 ng/μl, pTG96 at 100 ng/μl (Yochem et al., 1998) and pRF4 at 50 ng/μl (Mello et al., 1991); viable *ok3139* homozygotes were isolated and maintained from this strain.

RESULTS

Pharyngeal precursor cells form a bilaterally symmetric double plate

The pharynx forms from pharyngeal precursor cells (PPCs) that express PHA-4, a FoxA transcription factor essential for pharyngeal-specific differentiation (Fig. 1A) (Horner et al., 1998; Kalb et al., 1998; Mango et al., 1994). The PPCs are descendants of four early embryonic blastomeres (Fig. 1C) that are born on the ventral surface of the embryo, but after multiple cycles of cell division and ingression all PPCs are internalized (Fig. 1A) (Sulston et al., 1983). At ~400 minutes (timing from the first embryonic cell division), the PPCs undergo a MET to become a cylindrical cyst of polarized cells (Fig. 1A). Under electron microscopy, the cyst cells appear wedge shaped in transverse section, with narrow apical tips and broad peripheral surfaces (Leung et al., 1999).

For live imaging of cyst formation, we used a PPC-specific nuclear reporter (*pha-4*::HIS-GFP) and a ubiquitous plasma membrane reporter [*pie-1*::mCherry::PH(PLC1δ1), hereafter memb-mCherry]. Conventional mounting techniques for *C. elegans* embryos allow longitudinal optical sectioning (Fig. 1A,D).

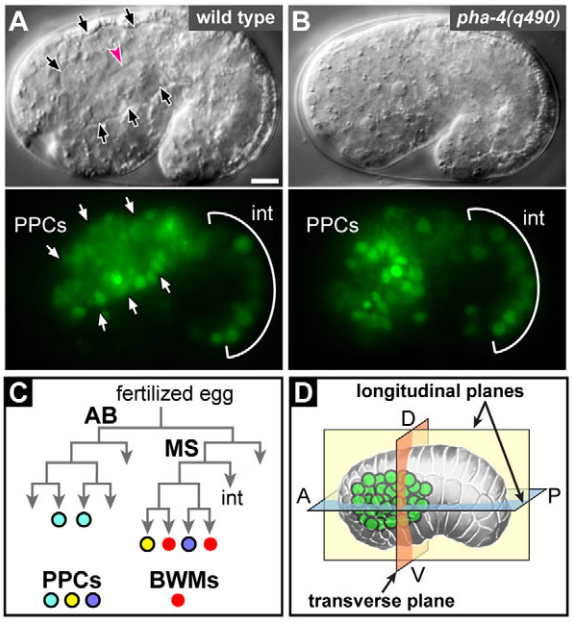

Fig. 1. Pharyngeal cyst development in wild-type and *pha-4* mutant *C. elegans* embryos. (**A**,**B**) Longitudinal optical sections through the centers of wild-type (A) and *pha-4(q490)* (B) embryos at ~420 minutes in development. Embryos express a nuclear reporter (*pha-4*::HIS-GFP, green) in all pharyngeal precursor cells (PPCs) and in intestinal cells (int). Because the PPC reporter does not encode the PHA-4 protein, it does not rescue the *pha-4* mutation and 'PPCs' in the mutant embryos do not differentiate as pharyngeal cells. Arrows in A indicate the periphery of the pharyngeal cyst and the red arrowhead indicates the developing apical lumen. (**C**) Partial cell lineage diagram indicating the origins of early cells described in this study. Body wall muscles (BWMs) are a non-pharyngeal type of muscle. (**D**) Optical sectioning planes used in this study superimposed on a depiction of an embryo midway through development. The internal position of the PPCs is indicated (green). D, dorsal; V, ventral; A, anterior; P, posterior. Scale bar: 5 μm.

However, this orientation compresses either the left-right or dorsal-ventral axis, and makes the wedge shapes of cyst cells difficult to score. Thus, we developed a technique to mount live embryos for transverse optical sectioning (Fig. 1D; see Materials and methods). We found that left and right PPCs at the ventral surface appear to sweep into the embryo interior from 150-260 minutes, converging into a dorsal-ventral-oriented rectangular array of cells (Fig. 2A). The array extends dorsally within the embryo as internal PPCs divide and additional PPCs ingress from the ventral surface. Although there are shifts in nuclear positions within the growing array, inspection of PPC boundaries showed that the array remains bilaterally symmetric and almost exclusively two cells wide. Thus, we term the array of PPCs the 'double plate' stage, and refer to the plane between the left and right halves of the double plate as the midplane (Fig. 2A, see also 2C).

We wanted to determine how bilateral symmetry is maintained during growth of the double plate. Previous studies have shown that most embryonic cell divisions are oriented longitudinally (anterior-posterior) rather than left-right, and that cell positions in the pharyngeal cyst and at later stages are correlated with the positions of some early PPCs (Santella et al., 2010; Sulston et al., 1983). Thus, bilateral symmetry of the double plate might derive simply from the original left-right positions of the PPCs and the subsequent anterior-posterior divisions of their descendants (Fig. 2C). Consistent with previous studies, we found that PPCs on the left and right sides of the double plate were the respective descendants of early left and right PPCs on the ventral surface of the embryo (Fig. 2C). In addition, we found that body wall muscles (BWMs) flank the left and right sides of the double plate PPCs, and precursors of the BWMs flank the left and right sides of the early PPCs (Fig. 2C,D). Although most PPC divisions in the double plate had the typical anterior-posterior orientation, we found that at least two PPCs consistently divided left-right (Fig. 2B). The left and right daughters of those PPCs remained on their respective sides of the midplane, indicating that the bilateral symmetry of the double plate is not maintained solely by an absence of left-right divisions.

We next addressed whether bilateral symmetry of the double plate might arise from a lack of PPC motility, thus maintaining early left-right differences in cell positions. We examined pharyngeal development in *mex-1(RNAi)* embryos that mislocalize the transcription factor SKN-1 (Bowerman et al., 1993). SKN-1 is required to specify the fate of an early blastomere called MS, the left and right daughters of which contribute to the left and right sides, respectively, of the double plate and flanking BWMs. In *mex-1* mutants, mislocalized SKN-1 can cause five embryonic cells to adopt MS-like fates and produce ectopic PPCs and BWMs (Mello et al., 1992). If PPCs simply remain in place after birth, *mex-1* mutants should form multiple islands of PPCs separated by BWMs. Instead, we found that terminal stage *mex-1(RNAi)* embryos usually formed a single block of pharyngeal cells without intervening BWMs (Fig. 2E). These results suggest that PPCs have an ability to move and aggregate with other PPCs.

We examined *wrm-1* mutants to ascertain whether cell fate differences between left and right PPCs contributed to the bilateral symmetry of the double plate. Previous studies showed that some gene expression differences between the left and right daughters of MS (MSa and MSp) and their respective descendants depend on the transcription factor POP-1/TCF and proteins that regulate POP-1 activity, such as WRM-1/β-catenin (Hermann et al., 2000; Rocheleau et al., 1999). We cultured temperature-sensitive *wrm-1(ne1982)* mutant embryos at the restrictive temperature (25°C) until after the left-right MS daughters were born, then downshifted the embryos to the permissive temperature (15°C) to follow the development of the PPCs. We found that MS daughters were born in their normal left-right positions and that the early descendants of both cells ingressed at the normal times. However, the border between the early left-right descendants quickly became more irregular than in wild-type embryos (Fig. 2F,G). At later stages, PPCs in control *wrm-1(ne1982)* embryos maintained at 15°C formed an apparently normal double plate (Fig. 2H), whereas PPCs in the temperature-shifted embryos formed an abnormal cluster that was more than two cells wide and remained ventral rather than extending dorsally (Fig. 2I).

Because the transcription factor PHA-4 (FoxA) is thought to be required for most, if not all, aspects of pharyngeal-specific differentiation (reviewed by Mango, 2009), we examined formation of the double plate in *pha-4(q490)* null mutants. We found that the timing and patterning of the early PPC divisions in *pha-4(q490)* embryos appeared similar to wild type (data not shown) and that all of the PPCs ingressed (Fig. 1B). After ingressing, the mutant PPCs assembled into an array that approximated the shape of the double plate and was surrounded by BWM precursors (Fig. 3B, 0′ panel; data not shown). However, the width of the array was more variable than in wild-type embryos, often with three or more cells dorsally and only one cell ventrally (Fig. 3A,B; supplementary

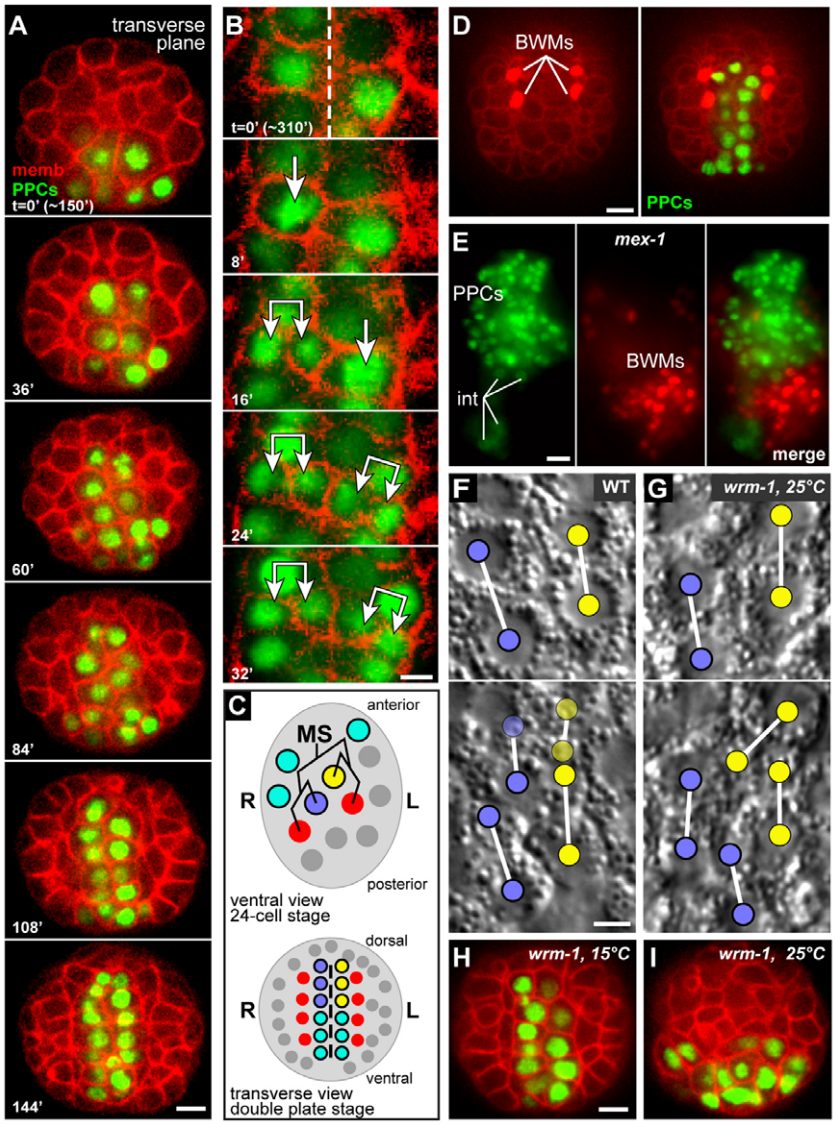

Fig. 2. PPCs organize into a bilaterally symmetric double plate. (**A**,**B**) Confocal fluorescence image sequence of single live *C. elegans* embryos expressing a PPC nuclear reporter (*pha-4*::HIS-GFP) and a membrane reporter (memb-mCherry). Images are transverse optical sections oriented as in Fig. 1D; images were collected ~15 μm from the anterior pole of the embryo. (A) PPCs are ingressing from the left and right ventral (bottom) surface of the embryo, then moving dorsally (top). By 290 minutes, the double plate is 6-8 cells deep. (B) Examples of left-right PPC divisions in the double plate. Cells are indicated before (single arrow) and after (double arrow) division. The dashed line indicates the midplane of the double plate. (**C**) Representation of the ventral surface of a 24-cell embryo (~100 minutes), and a transverse section through an embryo at the double plate stage (~290 minutes). Nuclei with bold outlines are PPCs and are color-coded as in Fig. 1C; red nuclei are BWM precursors. (**D**) Transverse optical section of a live ~250 minute embryo expressing the same PPC and membrane reporters as in A and B, but with an additional reporter for BWMs (*hlh-1*::HIS-mCherry). (**E**) Longitudinal optical section through a terminal stage *mex-1(RNAi)* embryo (anterior at top). Note the single large cluster of PPCs (green); the fainter, larger nuclei toward the bottom are intestinal nuclei (int). (**F**,**G**) Ventral surface views of live wild-type and *wrm-1(ts)* embryos raised at the restrictive temperature until MS cell division, then imaged at the permissive temperature. Images show before (top) and after (bottom) the fifth cell division of the MS-derived PPCs. Cells are color-coded as in Fig. 1C, with white lines indicating sister cells; cells that have ingressed are shown with lighter coloring. Note the irregular left-right positioning of cells in the *wrm-1(ts)* embryo. (**H**,**I**) Live *wrm-1(ts)* embryos raised at the permissive temperature (H) or temperature shifted (I) as in G; reporters and optical sectioning as in A. Note the failure of PPCs to form a double plate after shifting from the restrictive temperature (*n*=15/15 embryos). Scale bars: 5 μm in A,D,E,H,I; 2.5 μm in B,F,G.

material Movies 1, 2). Moreover, some PPCs crossed the midplane to the contralateral side (Fig. 3B; supplementary material Movie 2). At the cyst stage, wild-type PPCs become separated from other surrounding cells, including BWMs, by a laminin-containing basement membrane (Fig. 3C). By contrast, the *pha-4* mutant PPCs intermingled with both BWMs and unidentified surrounding cells without an intervening basement membrane (Fig. 3D). Together, these results indicate that the formation and maintenance of the double plate requires regulators of left-right differences and pharyngeal identity.

The double plate transforms into a cyst by apical constriction

The rectangular double plate of PPCs ultimately adopts the cylindrical shape of the cyst. A previous study based on nuclear PPC positions described the formation of the cyst as an inflation event that separated left from right groups of nuclei (Santella et al., 2010). Indeed, in transverse imaging of the double plate, many left and right PPC nuclei appeared to move apart from each other during cyst formation (330-390 minutes, Fig. 3A; supplementary material Movie 1). However, imaging of the cell membranes of PPCs showed that the nuclear movement occurs concomitant with changes in PPC shape (Fig. 4A,B). The midplane-facing surfaces of double plate PPCs shrink, whereas the peripheral surfaces show relatively little change in size (Fig. 4A,B,E). These changes result in radially elongated, wedge-shaped PPCs with nuclei that appear to be displaced toward the periphery by the shrinking midplane surface (Fig. 4A,B; supplementary material Movie 3). Thus, the midplane and peripheral surfaces of double plate PPCs become, respectively, the apical and basal surfaces of cyst PPCs.

In several systems, cells can adopt wedge-shaped morphology by apical constriction, which can be driven by the actomyosin cytoskeleton (reviewed by Sawyer et al., 2010). We found that reporters for non-muscle myosin and F-actin initially showed a slight and transient enrichment at the peripheral/basal surfaces of double plate PPCs. Thereafter, both reporters localized progressively to the midplane/apical surfaces as the PPCs developed wedge shapes (Fig. 4C-D′). Thus, the double plate appears to transform into the cyst by an asymmetric apical constriction.

In some epithelial tissues, including the *C. elegans* intestine, the asymmetric localization of centrosomes and of PAR-3 complex proteins are early markers of apical polarity (Buendia et al., 1990; Leung et al., 1999). To determine when double plate PPCs first become polarized, we scored the position of the centrosome in each

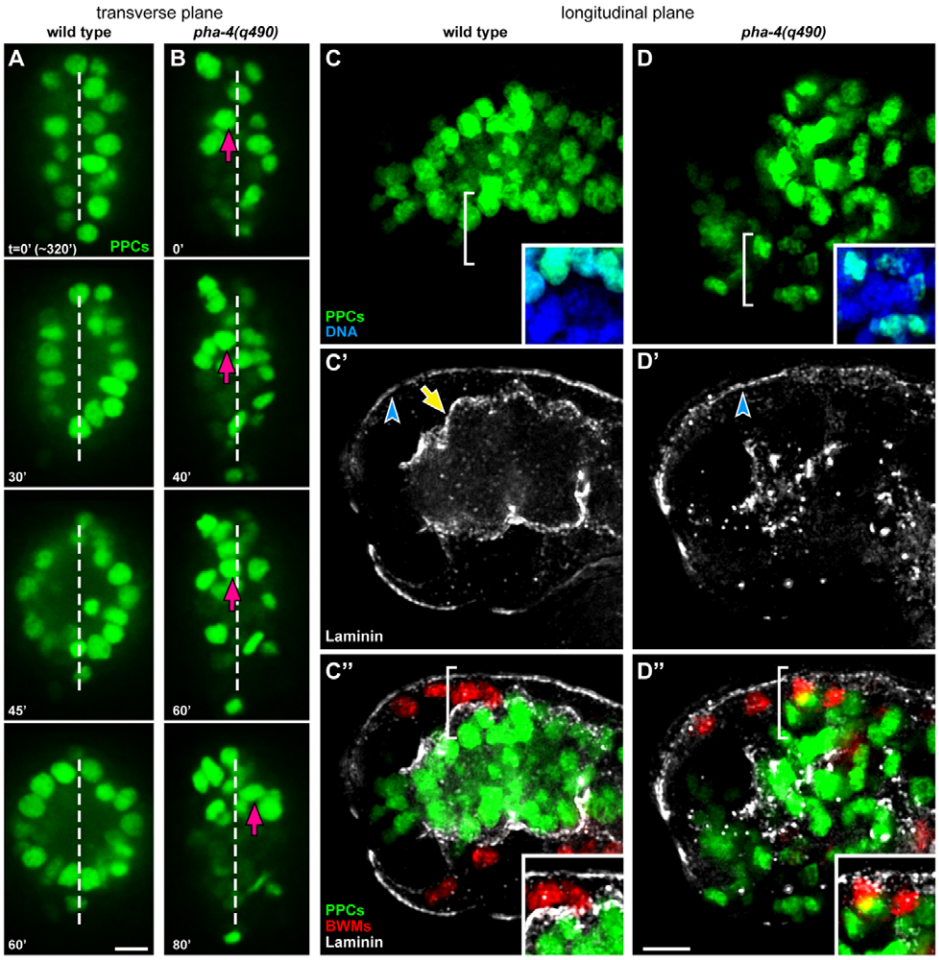

Fig. 3. PHA-4 shapes and maintains the double plate. (**A**) Transverse optical sections through a live wild-type *C. elegans* embryo showing the PPC (*pha-4*::HIS-GFP) transition from double plate to cyst. Images are from supplementary material Movie 1; the dashed line represents the midplane. (**B**) *pha-4(q490)* embryo showing PPCs inappropriately crossing the midplane (arrow) and the failure to form a cyst. Images are from supplementary material Movie 2. (**C-D″**) Longitudinal optical sections through the anterior of a fixed wild-type embryo and a *pha-4(q490)* mutant embryo immunostained as follows: PPC nuclei [anti-GFP (*pha-4*::HIS-GFP)], BWM nuclei (*hlh-1*::HIS-mCherry), laminin (mAbGJ2) and total nuclei (DAPI). Laminin outlines the body in both embryos (blue arrowhead). Laminin localizes to the periphery of the developing pharynx in the wild-type embryo (yellow arrow) and separates PPCs from the surrounding BWMs (see inset of bracketed region in C″). Note that laminin is present in an irregular pattern throughout the *pha-4* mutant PPCs (D′) and does not separate PPCs from BWMs (see inset of bracketed region in D″). The insets in C and D show merged images of PPC nuclei (green) and total nuclei (blue). Note that PPCs do not intermingle with non-PPCs in wild-type embryos, but mix in *pha-4* mutants. Time is in minutes. Scale bars: 5 μm.

PPC relative to the center of the nucleus, measuring whether the centrosome was proximal or distal to the midplane. Centrosomes initially showed an equal proximal-distal distribution, as expected from the predominantly anterior-posterior divisions of the PPCs (Fig. 4F). However, between ~290 and 310 minutes there was a shift in centrosome positions to face the midplane surfaces, before any apparent enrichment of non-muscle myosin or F-actin at the midplane (Fig. 4F). Similarly, proteins in the PAR-3 complex became enriched at the midplane prior to the non-muscle myosins NMY-1 and NMY-2 (Fig. 4G, Fig. 5A; data not shown). This difference in timing contrasts with the polarization of early one-cell and four-cell embryos, where the asymmetric localization of PAR-6 occurs simultaneously with NMY-2 (Munro et al., 2004).

Laminin orients polarity in double plate PPCs

In analyzing fixed, immunostained *mex-1(RNAi)* embryos, we noticed that ectopic PPCs at the embryo periphery (superficial PPCs) appeared to organize into cyst-like structures that were surrounded by laminin and that expressed lumen-specific apical markers (Fig. 6A; supplementary material Fig. S1). In live recordings, we found that the cyst-like structures developed from PPCs that were born, and remained, at the periphery of the *mex-1(RNAi)* embryos (Fig. 6B). These superficial PPCs lacked direct contact with BWMs or other non-PPCs, but localized PAR-6 to their interior or apical surfaces and appeared to undergo at least some apical constriction (Fig. 6B; supplementary material Movie 5). These results suggest that PPC polarization does not require direct cell contact with non-PPCs and might involve diffusible signals.

Because in vitro studies suggest that the secreted protein laminin functions as a polarizing cue for MDCK cells (see Introduction), we immunostained fixed wild-type embryos for PAR-3 and either LAM-3/laminin α or PAT-3/β-integrin, a candidate laminin receptor. We found that all three proteins were present in double plate PPCs, and all showed asymmetry at about the same stage; PAR-3 localized to the midplane/apical surfaces and LAM-3 and PAT-3 localized to the peripheral/basal surfaces (Fig. 5D,E). Similarly, live recordings of separate embryos expressing reporters for PAR-6, laminin or β-integrin showed asymmetric localization at similar developmental stages (Fig. 5A-C). We next constructed a strain that expressed both mCherry::PAR-6 and LAM-1::GFP and found that basal enrichment of LAM-1 preceded apical enrichment of PAR-6 by at least 15 minutes (Fig. 5F; supplementary material Movie 6).

To determine whether laminin has a role in polarizing the double plate PPCs, we examined embryos homozygous for *lam-1(ok3139)*, a predicted null mutation in the sole laminin β subunit (supplementary material Fig. S2; see Materials and methods). *lam-1(–)* embryos have abnormal pharyngeal basement membranes but localize at least some basement membrane components (supplementary material Fig. S3). Although *lam-1(–)* embryos appear highly abnormal by light microscopy, they appear to produce all of the major differentiated tissue types (Fig. 7A,B), consistent with previous studies on other mutations in laminin subunits (Huang et al., 2003; Kao et al., 2006). In particular, differentiated pharyngeal tissue contained internal lines of material resembling the normal cuticle-lined pharyngeal lumen. Remarkably, however, the

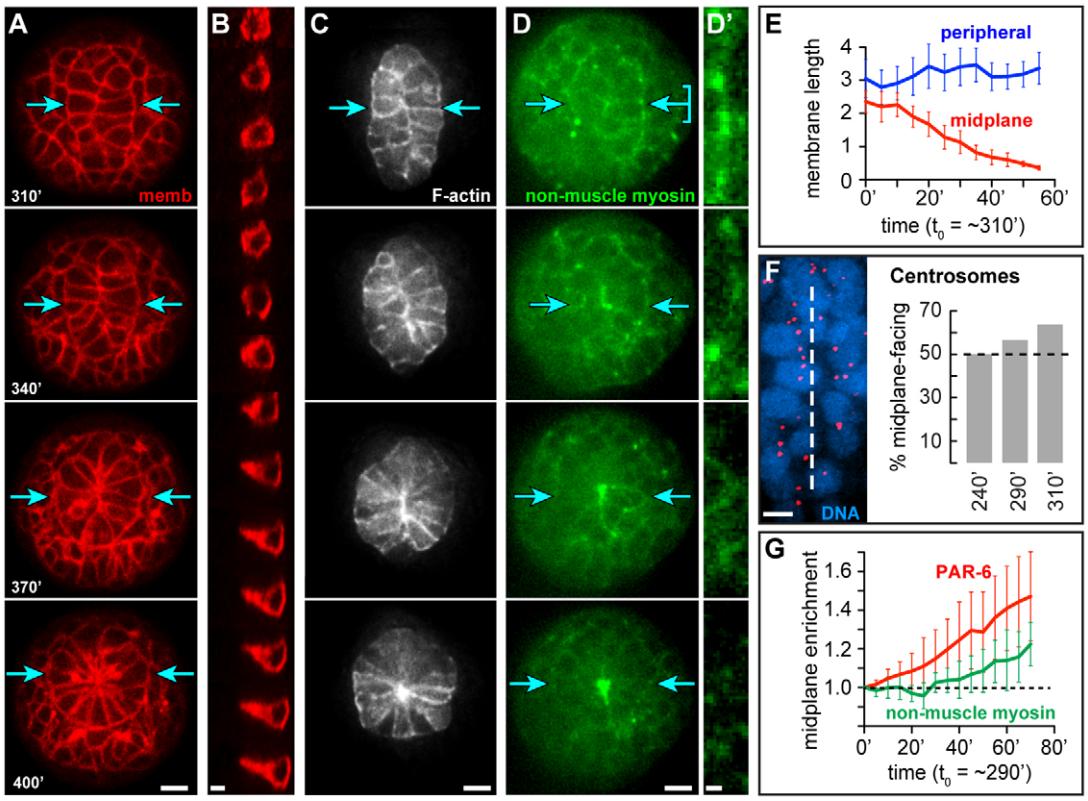

Fig. 4. Cyst formation by apical constriction of double plate PPCs. (**A-D'**) Transverse optical sections of live *C. elegans* embryos showing the transition from double plate to cyst. Arrows at the first time point indicate the left and right margins of the double plate. (A) Image sequence from supplementary material Movie 3 showing all cell membranes (memb-mCherry). (B) Image sequence showing cell shape changes for a single PPC marked by *zuEx254*, which is expressed in only a few PPCs. (C) F-actin expression (*pha-4*::GFP::dMoesin-ABD) in the PPCs. Note the enrichment along the midplane/apical surface. (D) Non-muscle myosin expression (*nmy-2*::NMY-2::GFP). (D') High magnification of the periphery of the double plate (arrow with bracket in D). Note that non-muscle myosin is initially enriched at the periphery of PPCs, but disappears from the periphery as it concentrates apically. (**E**) Average membrane length (μm) of midplane and peripheral PPC surfaces. Error bars indicate 95% confidence intervals. (**F**) The left panel is a longitudinal view (anterior at top) of the double plate PPCs (DAPI , blue) at ~310 minutes showing the positions of centrosomes (IFA, red) relative to the midplane (dashed line). Note the number of midplane-facing centrosomes. The right panel quantifies centrosome positions over time (n>55 centrosomes per time point). (**G**) Quantification of midplane enrichment of PAR-6 (*pie-1*::mCherry::PAR-6) and NMY-2 (*nmy-2*::NMY-2::GFP) in single embryos expressing both reporters (n=4 embryos). See also supplementary material Movie 4. Error bars indicate 95% confidence intervals. Scale bars: 5 μm in A,C,D; 2.5 μm in B,F; 1 μm in D'.

lam-1(–) pharynx usually contained two or more such lines (Fig. 7B; n=96/97 embryos); transverse imaging showed that the supernumerary lines were not simply aberrant radial outgrowths from the single normal lumen, but instead appeared to be separate lumens (Fig. 7C,D). Interestingly, the intestine developed a single lumen in *lam-1(–)* mutants (Fig. 7E,F), consistent with our observation that proteins in the PAR-3 complex localize to the apical surfaces of intestinal cells before laminin is detectable at the basal surfaces (J. Feldman and J.R.P., unpublished). The multi-lumen pharyngeal defect did not result from a hyperplasia of pharyngeal tissue as the mutant embryos contained the wild-type number of PPCs (88±2, n=4 embryos) (Kalb et al., 1998). Null mutants in single laminin α subunits [*lam-3(n2561)* or *epi-1(rh199)*], in the basement membrane components perlecan [*unc-52(st549)*] or in type IV collagen [*emb-9(g23cg46)*] had widespread defects in tissue morphology, but did not exhibit the multi-lumen defect (Fig. 7G-J). Thus, laminin appears to have a specific role in specifying the single lumen of the wild-type pharynx.

To determine the ontogeny of the multi-lumen pharyngeal defect, we examined PAR-3 and PAR-6 localization in live and fixed *lam-1(–)* embryos. PPCs in the *lam-1(–)* embryos organized into a double plate that appeared similar in morphology to the wild-type double plate (supplementary material Movie 9). Surprisingly, however, many of the mutant PPCs showed inverted polarity and localized PAR-3 and PAR-6 to the peripheral/basal surfaces at the same time that these proteins normally localize to the midplane/apical surfaces (Fig. 8A-D; supplementary material Movies 7, 8). With simultaneous imaging of PAR-6 and a general membrane reporter, we confirmed that the peripheral PAR-6 was within the mutant PPCs rather than in adjacent BWMs (Fig. 8E,F). We considered the possibility that the inverted polarity of the PPCs might result from inappropriate interactions with neighboring non-PPCs, which normally are separated by the basement membrane. However, we found that the superficial PPCs in *mex-1(RNAi); lam-1(–)* embryos showed a similar inverted polarity, with PAR-3 localized primarily to the peripheral, contact-free surfaces (Fig. 6C).

We found that the multi-lumen pharyngeal defect of terminal stage *lam-1(–)* embryos results from cell movements that internalize the peripheral surfaces of PPCs. Live imaging of *lam-1(–)* embryos expressing reporters for cell membranes and either PAR-6 or non-muscle myosin showed that the peripheral surfaces

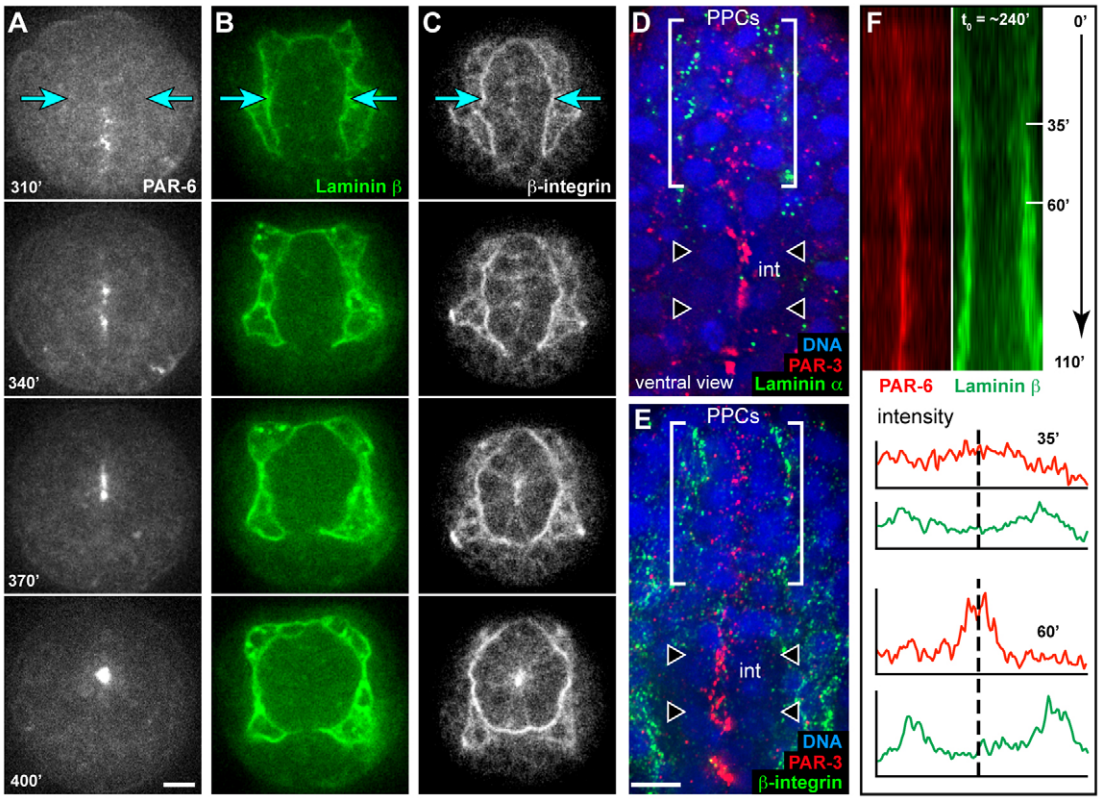

Fig. 5. Onset of apical and basal polarity in double plate PPCs. (**A-C**) Transverse optical sections of live *C. elegans* embryos showing the transition from double plate to cyst. Arrows indicate the left and right margins of the double plate. Embryos express the following reporters: (A) PAR-6 (*pie-1*::mCherry::PAR-6), (B) laminin β (*lam-1*::LAM-1::GFP) and (C) β-integrin (*pat-3*::PAT-3::GFP). See supplementary material Movie 6 for onset of *lam-1*::LAM-1::GFP expression. (**D**,**E**) Longitudinal optical sections through the center of the double plate (brackets) and intestine (int, arrowheads). The embryos were immunostained for PAR-3 and either laminin α (mAbGJ1) (D) or β-integrin (MH25) (E). The embryos were selected for the earliest detectable asymmetry of PAR-3 in the PPCs. Note that at this stage both laminin α and β-integrin are enriched in puncta at the periphery of the double plate; at later stages, laminin α and β-integrin uniformly coat the basal PPC surfaces (see Fig. 3C″; supplementary material Fig. S4). LAM-3 is not enriched at the periphery of the intestinal cells (arrowheads). (**F**) Kymograph analysis (top) from supplementary material Movie 6 of an embryo co-expressing *pie-1*::mCherry::PAR-6 and *lam-1*::LAM-1::GFP showing the width of the double plate and surrounding BWMs. Beneath are shown fluorescence intensity line scans across the kymographs at 35 and 60 minutes. The dashed line indicates the midplane. Scale bars: 5 μm.

of several PPCs constricted at about the same time as the midplane surfaces normally constrict in wild-type PPCs (Fig. 8G-G″; supplementary material Movies 8, 9). Neighboring PPCs spread across and enclosed the peripheral constrictions, which underwent lumenal differentiation. We conclude that *lam-1(–)* mutants have an early and highly penetrant defect in orienting PPC polarity that is partially masked by subsequent morphogenetic movements.

Laminin can act non-cell-autonomously to orient PPC polarity

Because several *C. elegans* tissues have been reported to express laminin, including the pharynx, intestine and BWMs (Huang et al., 2003; Kao et al., 2006), we investigated which cells must express *lam-1* to properly orient PPC polarity. We constructed a homozygous *lam-1(ok3139)* strain that carried an extrachromosomal array (*zuEx288*) containing a wild-type *lam-1(+)* gene plus a cell-autonomous marker (SUR-5::GFP); such transgenic arrays are lost stochastically during cell divisions, resulting in animals that are mosaic for gene expression. As expected, animals that lacked *zuEx288* had the multi-lumen defect (n=60/61), whereas animals that had *zuEx288* in most or all cells had a normal pharynx with a single lumen (Fig. 7K; n=46/47). We then searched for rare mosaic animals that lacked *zuEx288* in all pharyngeal cells but that retained the transgene in other cell groups. We found that the pharynx had a single lumen in 6/8 animals with *zuEx288* only in intestinal cells (Fig. 7L) and in 14/17 animals with *zuEx288* only in skin (hypodermal) cells and BWMs (Fig. 7M). These results suggest that laminin expressed by non-PPCs diffuses through the embryo and accumulates on the available basal surface of PPCs where it acts as a polarity cue.

DISCUSSION

Morphogenesis of the pharyngeal cyst proceeds through a distinct, bilaterally symmetric intermediate termed the double plate, where PPCs first develop apical/basal polarity. The mature *C. elegans* pharynx has threefold symmetry, but has an underlying bilateral symmetry evident in the cell lineages of MS descendants that produce about half of the pharynx (Albertson and Thomson, 1976; Sulston et al., 1983). For example, symmetrical and identical cells in the mature pharynx called mc3DL and mc3DR are descendants of the left and right daughters of MS, respectively, and their fates appear to be determined by a lineage mechanism rather than cell position (Priess et al., 1987). These cells do not contact each other in the mature pharynx and are separated from their nearest common

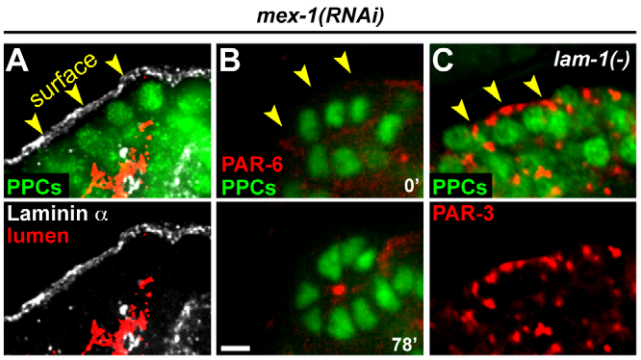

Fig. 6. PPC polarity in *mex-1* embryos. (**A**) High-magnification view of superficial PPCs in a *mex-1(RNAi) C. elegans* embryo. The embryo was immunostained for laminin α (mAbGJ1), PPCs [anti-GFP (*pha-4*::PHA-4::GFP)] and a lumenal marker (mAbPL1). Note that laminin accumulates at the external, contact-free periphery of the superficial PPCs (arrowheads) and that lumenal markers differentiate one cell diameter inward from the periphery, similar to the wild-type cyst. (**B**) Images from supplementary material Movie 5 of superficial PPCs in a live *mex-1(RNAi)* embryo expressing reporters for PAR-6 (*pie-1*::mCherry::PAR-6) and PPC nuclei (*pha-4*::PHA-4::GFP). Note the accumulation of PAR-6 at the center of a cyst-like structure. (**C**) Superficial PPCs in a *mex-1(RNAi); lam-1(ok3139)* embryo immunostained for PAR-3 and PPC nuclei [anti-GFP (*pha-4*::PHA-4::GFP)]. Note that in the absence of laminin, PAR-3 accumulates with inverted polarity on the contact-free surface. Time is in minutes. Scale bar: 2.5 μm.

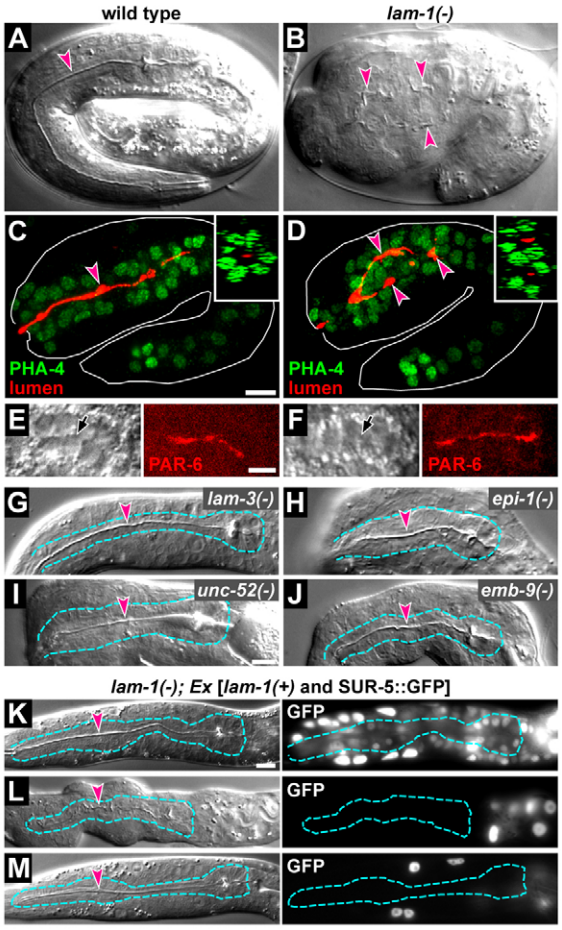

Fig. 7. Laminin is required to specify the single pharyngeal lumen. (**A**,**B**) Brightfield images of late stage wild-type and *lam-1(ok3139) C. elegans* embryos. Arrowheads indicate the cuticle-lined pharyngeal lumen. Note the multiple lumens in the *lam-1(–)* mutant. (**C**,**D**) Immunostained wild-type and *lam-1(–)* embryos at 470 minutes showing PPC nuclei [anti-GFP (*pha-4*::PHA-4::GFP)] and a marker for the pharyngeal lumen (mAbPL1). Insets are reconstructed transverse views through the pharynx. Note that both of the apparent lumens in the *lam-1(–)* embryo are surrounded by PPCs. (**E**,**F**) Brightfield and fluorescent images of the intestine in live wild-type and *lam-1(–)* embryos at ~280 minutes, showing localization of PAR-6 (*par-6*::PAR-6::GFP) to a single lumen (arrow). Although *lam-1(–)* embryos showed some mispositioning of intestinal cells, each of 28 embryos examined localized PAR-3 or PAR-6 only to the apical surfaces of intestinal cells. (**G-J**) Brightfield images of newly hatched larvae showing a single internal pharyngeal lumen in null mutants for LAM-3/laminin α (G), EPI-1/laminin α (H), UNC-52/perlecan (I) and EMB-9/type IV collagen (J). *n*>50 animals examined for each genotype. The pharynx is outlined (blue dashed line). (**K-M**) Newly hatched homozygous *lam-1(–)* mutant larvae that are mosaic for LAM-1 expression [*zuEx288: lam-1(+)* transgene marked by *sur-5*::SUR-5::GFP]. Note the formation of a single pharyngeal lumen (arrowhead) when *zuEx288* is present only in the intestine (L) or in hypodermis and BWMs (M). Scale bars: 5 μm.

ancestor by seven cell divisions. How then are these cells able to occupy precisely symmetrical positions? We suggest that the double plate structure allows specific pairs of left and right precursor cells to maintain, and possibly adjust, their proximity throughout the early stages of pharynx formation, until they are physically separated by cyst morphogenesis.

Two lines of evidence suggest that PPCs actively aggregate into the double plate primordium. First, ectopic supernumerary PPCs in *mex-1* mutants can form a single block of pharyngeal cells that excludes other cell types such as BWMs and intestinal cells. Second, PPCs lacking PHA-4, the master regulator of pharyngeal-specific differentiation, can intermingle with non-PPCs. The bilateral symmetry of the double plate is likely to involve differential cell adhesion because left and right PPCs stay on their respective sides as the double plate grows, even when these PPCs are born through left-right cell divisions. We showed that *wrm-1*, an integral component of the POP-1/TCF pathway (Rocheleau et al., 1999), is required for the rectangular shape and bilateral symmetry of the double plate. The POP-1/TCF pathway operates in the early embryo to create numerous differences between anterior-posterior sister cells (reviewed by Herman and Wu, 2004). However, because the division axes of most early cells are oblique, many anterior-posterior sisters differ in their left-right positions, resulting in left-right differences in gene expression. For example, only left descendants of the MS blastomere express the Notch ligand LAG-2/Delta, but both left and right descendants can express this protein when the POP-1/TCF pathway is disrupted (Hermann et al., 2000). Thus, analogous left-right differences in early cell adhesion could shape the double plate, and an important goal of future studies will be to identify the molecular basis for those differences.

The double plate transforms into a cylindrical cyst, apparently by PPCs constricting their midplane, or apical, surfaces (Fig. 9); the apical surfaces decrease in size concomitant with an increase in F-actin and non-muscle myosin. The basal surfaces of the PPCs show relatively little change in size during apical constriction, suggesting that these surfaces might adhere to neighboring cells or extracellular matrix. We showed that the PPCs are surrounded by laminin before constriction, that they express the candidate laminin receptor PAT-3, and that the basal surface can change size markedly in laminin mutants with inverted PPC polarity.

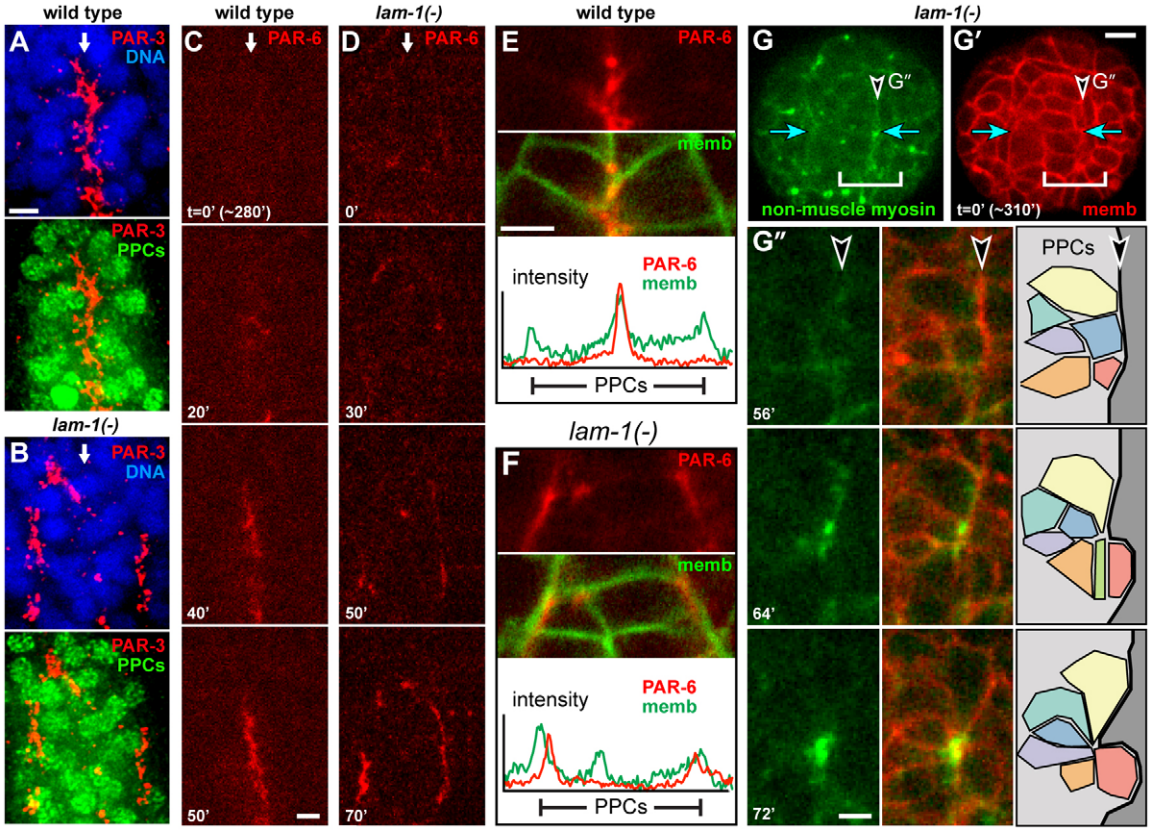

Fig. 8. Laminin cues PPC polarity. (**A**,**B**) Longitudinal optical sections through the double plate PPCs of immunostained wild-type and *lam-1(ok3139) C. elegans* embryos. Anterior is top. Images show PPC nuclei [anti-GFP (*pha-4*::PHA-4::GFP)], total nuclei (DAPI) and PAR-3 as maximum intensity projections through the double plate; arrows indicate the midplane. Note that PAR-3 localizes to midplane surfaces in the wild-type double plate, but predominantly to peripheral surfaces in the *lam-1(–)* embryo [*n*>50 for wild type; *n*=18/18 for *lam-1(–)*]. (**C**,**D**) Optical sections as in A and B of live embryos expressing a PAR-6 reporter (*par-6*::PAR-6::GFP). Note that PAR-6 localization begins, and persists, at the peripheral surfaces of the double plate in the *lam-1(–)* embryos (*n*=16/16). See supplementary material Movies 7 and 8 for cell membranes of PPCs. (**E**,**F**) High-magnification images of part of a longitudinal optical section through the double plate of live wild-type (E) and *lam-1(–)* (F) embryos showing PAR-6 (*par-6*::PAR-6::GFP) and plasma membranes (memb-mCherry). Line scans through the double plate are shown beneath each image. Note that ectopic PAR-6 is localized within the PPCs in the *lam-1(–)* embryo. (**G-G″**) Images from supplementary material Movie 9 showing transverse optical sections of a live *lam-1(–)* embryo expressing reporters for non-muscle myosin (*nmy-2*::NMY-2::GFP) and plasma membranes (memb-mCherry). Images in G″ are high-magnification views of PPCs at the periphery of the double plate (arrowhead and bracketed region in G and G′). The diagrams show tracings of individual color-coded PPCs within the double plate (light gray region), taken from movie frames at left. Time is in minutes. Scale bars: 2.5 μm in A-F,G″; 5 μm in G.

The coordinated polarization of large groups of cells is a hallmark of epithelial development that allows tubular epithelia to form a single, continuous lumen. Our results show that laminin provides a crucial cue for the coordinate polarization of epithelial cells in the pharynx, although not for epithelial cells in the intestine. A previous study showed that *C. elegans* mutants lacking LAM-3, one of two laminin α subunits, develop ruptures in the pharyngeal basement membrane and that some pharyngeal cells appear to adhere to surrounding tissues through these gaps (Huang et al., 2003). However, all of the mutant pharyngeal cells appeared to connect to a central lumen, as do the wild-type pharyngeal cells. Although pharyngeal cells lacking LAM-1, the sole laminin β subunit, similarly connect to a lumenal surface, we showed that there are multiple lumenal surfaces in the mutant pharynx and that these arise from polarity defects in double plate PPCs. The double plate PPCs polarize abnormally in *lam-1* mutants, with many localizing PAR-3 and PAR-6 to their peripheral (normally basal) surfaces. Remarkably, these peripheral surfaces can constrict, like the normal apical surface, and become repositioned into the interior of the developing pharynx by the neighboring PPCs. These polarity defects occur at least an hour before perlecan and type IV collagen localize to the wild-type pharyngeal basement membrane (Graham et al., 1997; Mullen et al., 1999) and were not observed in mutants for either basement membrane component. Thus, we propose that the defects represent a specific requirement for laminin in PPC polarization, rather than general functions of the basement membrane in tissue integrity.

Several embryonic cell types, including PPCs, normally express laminin. Our analysis of laminin mosaics shows that laminin supplied by non-PPCs is sufficient to orient PPC polarity. Consistent with previous observations on laminin and type IV collagen, this result suggests that basement membrane components can diffuse through the embryo (Graham et al., 1997; Huang et al., 2003). We presume that PPC adhesion, as evidenced by the aggregation of supernumerary PPCs in *mex-1(RNAi)* embryos, normally restricts laminin to the peripheral surface of the double plate. PPCs do not appear to maintain normal adhesion in *pha-4* mutants, and we showed that laminin distributes in an irregular

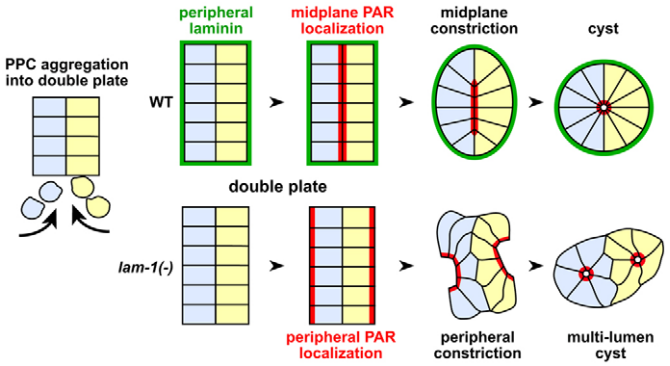

Fig. 9. Model of cyst morphogenesis in *C. elegans*. Summary of the formation of the pharyngeal cyst (transverse views). Left (yellow) and right (light blue) PPCs ingress from the ventral (bottom) surface of the embryo and aggregate to form the bilaterally symmetric double plate. Laminin accumulates on the exposed peripheral surface of the double plate in wild-type embryos, but is absent in *lam-1(–)* embryos. Laminin at the peripheral surface precedes, and is required for, localization of proteins in the PAR-3 complex to the opposite, midplane surface. In *lam-1* mutants, PAR proteins accumulate ectopically on the peripheral surface. Cell surface constriction occurs where PAR proteins localize, leading to midplane constriction in wild-type embryos and the formation of a single-lumen cyst. In *lam-1* mutants, peripheral constriction and shifts in PPC position internalize the PAR-containing peripheral surfaces, leading to a multi-lumen cyst.

pattern between the mutant PPCs. We have no evidence that laminin receptors are localized to the peripheral surfaces of double plate PPCs prior to laminin enrichment. Indeed, we found that PAT-3 localizes to the basal surface at about the same time as laminin, and that laminin function is required for PAT-3 localization (supplementary material Fig. S4). We do not yet know whether PAT-3 is required to orient the midplane/apical localization of the PAR-3 complex: embryos homozygous for a null *pat-3* mutation expressed PAT-3, suggesting that *pat-3* mRNA is contributed from the heterozygous mother, and exposing the mothers to *pat-3* dsRNA resulted in early embryonic arrest that precluded analysis of the pharynx (data not shown).

In *Drosophila*, similar to *C. elegans*, some laminin subunits are encoded by single genes; however, the respective *Drosophila* mutants do not exhibit defects in coordinating epithelial polarity (Urbano et al., 2009). Thus, laminin could function as a polarity signal in only certain epithelia, such as the pharynx, or might function redundantly with other signals such as other basement membrane proteins. Alternatively, later morphogenetic movements could obscure early polarity defects, as we demonstrated in the *C. elegans* pharynx. A third possibility is that some epithelia recognize inappropriate features of their environment as polarity cues when laminin is absent. By analogy, when the sperm-supplied centrosome is not available to polarize the one-cell *C. elegans* embryo, the meiotic spindle at the opposite pole of the egg appears to cue an inverted polarity (Wallenfang and Seydoux, 2000). Similarly, *Drosophila* wing epithelial cells polarize in the absence of planar cell polarity components, but fail to coordinate their polarity at the tissue level (Wong and Adler, 1993). Basement membrane defects in laminin mutants might allow some PPCs to make inappropriate contacts with surrounding tissues. However, we do not believe that those tissues induce the inversion of an otherwise normal PPC polarity because superficial PPCs in *mex-1(RNAi); lam-1(–)* embryos that do not contact any non-PPCs nevertheless develop inverted polarity. Thus, the present study provides in vivo evidence that laminin acts as a polarizing cue for some, although not all, epithelia. We conclude that the *C. elegans* pharynx should provide a useful genetic model for dissecting laminin-based signaling prior to the general requirements for laminin in basement membrane assembly and tissue integrity.

Acknowledgements
We thank James Kramer, Susan Mango, Donald Moerman, John Murray, Jeremy Nance, Alisa Piekny, William Wadsworth and the Developmental Studies Hybridoma Bank for providing antisera/strains and members of the J.R.P. lab for valuable discussions. Some strains used in this study were obtained from the *Caenorhabditis* Genetics Center, which is supported by the NIH National Center for Research Resources.

Funding
This work was supported by a Developmental Biology Predoctoral Training Grant from the National Institute of Child Health and Human Development [T32HD007183 to J.P.R.]; the NIH [R01GM098583 to J.R.P.]; and Howard Hughes Medical Institute (to J.R.P.). Deposited in PMC for release after 6 months.

Competing interests statement
The authors declare no competing financial interests.

Supplementary material
Supplementary material available online at
http://dev.biologists.org/lookup/suppl/doi:10.1242/dev.078360/-/DC1

References

Achilleos, A., Wehman, A. M. and Nance, J. (2010). PAR-3 mediates the initial clustering and apical localization of junction and polarity proteins during C. elegans intestinal epithelial cell polarization. *Development* **137**, 1833-1842.
Albertson, D. G. and Thomson, J. N. (1976). The pharynx of Caenorhabditis elegans. *Philos. Trans. R. Soc. Lond. B Biol. Sci.* **275**, 299-325.
Aumailley, M., Bruckner-Tuderman, L., Carter, W. G., Deutzmann, R., Edgar, D., Ekblom, P., Engel, J., Engvall, E., Hohenester, E., Jones, J. C. et al. (2005). A simplified laminin nomenclature. *Matrix Biol.* **24**, 326-332.
Bossinger, O., Klebes, A., Segbert, C., Theres, C. and Knust, E. (2001). Zonula adherens formation in Caenorhabditis elegans requires dlg-1, the homologue of the Drosophila gene discs large. *Dev. Biol.* **230**, 29-42.
Bowerman, B., Draper, B. W., Mello, C. C. and Priess, J. R. (1993). The maternal gene skn-1 encodes a protein that is distributed unequally in early C. elegans embryos. *Cell* **74**, 443-452.
Brenner, S. (1974). The genetics of Caenorhabditis elegans. *Genetics* **77**, 71-94.
Buendia, B., Bré, M. H., Griffiths, G. and Karsenti, E. (1990). Cytoskeletal control of centrioles movement during the establishment of polarity in Madin-Darby canine kidney cells. *J. Cell Biol.* **110**, 1123-1135.
Chaffer, C. L., Thompson, E. W. and Williams, E. D. (2007). Mesenchymal to epithelial transition in development and disease. *Cells Tissues Organs* **185**, 7-19.
Ekblom, P. (1989). Developmentally regulated conversion of mesenchyme to epithelium. *FASEB J.* **3**, 2141-2150.
Francis, G. R. and Waterston, R. H. (1985). Muscle organization in Caenorhabditis elegans: localization of proteins implicated in thin filament attachment and I-band organization. *J. Cell Biol.* **101**, 1532-1549.
Graham, P. L., Johnson, J. J., Wang, S., Sibley, M. H., Gupta, M. C. and Kramer, J. M. (1997). Type IV collagen is detectable in most, but not all, basement membranes of Caenorhabditis elegans and assembles on tissues that do not express it. *J. Cell Biol.* **137**, 1171-1183.
Gupta, M. C., Graham, P. L. and Kramer, J. M. (1997). Characterization of alpha1(IV) collagen mutations in Caenorhabditis elegans and the effects of alpha1 and alpha2(IV) mutations on type IV collagen distribution. *J. Cell Biol.* **137**, 1185-1196.
Hagedorn, E. J., Yashiro, H., Ziel, J. W., Ihara, S., Wang, Z. and Sherwood, D. R. (2009). Integrin acts upstream of netrin signaling to regulate formation of the anchor cell's invasive membrane in C. elegans. *Dev. Cell* **17**, 187-198.
Herman, M. A. and Wu, M. (2004). Noncanonical Wnt signaling pathways in C. elegans converge on POP-1/TCF and control cell polarity. *Front. Biosci.* **9**, 1530-1539.
Hermann, G. J., Leung, B. and Priess, J. R. (2000). Left-right asymmetry in C. elegans intestine organogenesis involves a LIN-12/Notch signaling pathway. *Development* **127**, 3429-3440.
Horner, M. A., Quintin, S., Domeier, M. E., Kimble, J., Labouesse, M. and Mango, S. E. (1998). pha-4, an HNF-3 homolog, specifies pharyngeal organ identity in Caenorhabditis elegans. *Genes Dev.* **12**, 1947-1952.
Huang, C. C., Hall, D. H., Hedgecock, E. M., Kao, G., Karantza, V., Vogel, B. E., Hutter, H., Chisholm, A. D., Yurchenco, P. D. and Wadsworth, W. G.

(2003). Laminin alpha subunits and their role in C. elegans development. *Development* **130**, 3343-3358.
Kachur, T. M., Audhya, A. and Pilgrim, D. B. (2008). UNC-45 is required for NMY-2 contractile function in early embryonic polarity establishment and germline cellularization in C. elegans. *Dev. Biol.* **314**, 287-299.
Kalb, J. M., Lau, K. K., Goszczynski, B., Fukushige, T., Moons, D., Okkema, P. G. and McGhee, J. D. (1998). pha-4 is Ce-fkh-1, a fork head/HNF-3alpha,beta,gamma homolog that functions in organogenesis of the C. elegans pharynx. *Development* **125**, 2171-2180.
Kamath, R. S., Fraser, A. G., Dong, Y., Poulin, G., Durbin, R., Gotta, M., Kanapin, A., Le Bot, N., Moreno, S., Sohrmann, M. et al. (2003). Systematic functional analysis of the Caenorhabditis elegans genome using RNAi. *Nature* **421**, 231-237.
Kao, G., Huang, C. C., Hedgecock, E. M., Hall, D. H. and Wadsworth, W. G. (2006). The role of the laminin beta subunit in laminin heterotrimer assembly and basement membrane function and development in C. elegans. *Dev. Biol.* **290**, 211-219.
Klein, G., Langegger, M., Timpl, R. and Ekblom, P. (1988). Role of laminin A chain in the development of epithelial cell polarity. *Cell* **55**, 331-341.
Leung, B., Hermann, G. J. and Priess, J. R. (1999). Organogenesis of the Caenorhabditis elegans intestine. *Dev. Biol.* **216**, 114-134.
Maduro, M. and Pilgrim, D. (1995). Identification and cloning of unc-119, a gene expressed in the Caenorhabditis elegans nervous system. *Genetics* **141**, 977-988.
Mango, S. (2009). The molecular basis of organ formation: insights from the C. elegans foregut. *Annu. Rev. Cell Dev. Biol.* **25**, 597-628.
Mango, S. E., Lambie, E. J. and Kimble, J. (1994). The pha-4 gene is required to generate the pharyngeal primordium of Caenorhabditis elegans. *Development* **120**, 3019-3031.
Marinkovich, M. P. (2007). Tumour microenvironment: laminin 332 in squamous-cell carcinoma. *Nat. Rev. Cancer* **7**, 370-380.
McMahon, L., Legouis, R., Vonesch, J. L. and Labouesse, M. (2001). Assembly of C. elegans apical junctions involves positioning and compaction by LET-413 and protein aggregation by the MAGUK protein DLG-1. *J. Cell Sci.* **114**, 2265-2277.
Mello, C. C., Kramer, J. M., Stinchcomb, D. and Ambros, V. (1991). Efficient gene transfer in C.elegans: extrachromosomal maintenance and integration of transforming sequences. *EMBO J.* **10**, 3959-3970.
Mello, C. C., Draper, B. W., Krause, M., Weintraub, H. and Priess, J. R. (1992). The pie-1 and mex-1 genes and maternal control of blastomere identity in early C. elegans embryos. *Cell* **70**, 163-176.
Miner, J. H. and Yurchenco, P. D. (2004). Laminin functions in tissue morphogenesis. *Annu. Rev. Cell Dev. Biol.* **20**, 255-284.
Miner, J. H., Cunningham, J. and Sanes, J. R. (1998). Roles for laminin in embryogenesis: exencephaly, syndactyly, and placentopathy in mice lacking the laminin alpha5 chain. *J. Cell Biol.* **143**, 1713-1723.
Mörck, C., Axäng, C. and Pilon, M. (2003). A genetic analysis of axon guidance in the C elegans pharynx. *Dev. Biol.* **260**, 158-175.
Mullen, G., Rogalski, T., Bush, J., Gorji, P. and Moerman, D. (1999). Complex patterns of alternative splicing mediate the spatial and temporal distribution of perlecan/UNC-52 in Caenorhabditis elegans. *Mol. Biol. Cell* **10**, 3205-3221.
Munro, E., Nance, J. and Priess, J. R. (2004). Cortical flows powered by asymmetrical contraction transport PAR proteins to establish and maintain anterior-posterior polarity in the early C. elegans embryo. *Dev. Cell* **7**, 413-424.
Murray, J. I., Bao, Z., Boyle, T. J., Boeck, M. E., Mericle, B. L., Nicholas, T. J., Zhao, Z., Sandel, M. J. and Waterston, R. H. (2008). Automated analysis of embryonic gene expression with cellular resolution in C. elegans. *Nat. Methods* **5**, 703-709.
Nakamura, K., Kim, S., Ishidate, T., Bei, Y., Pang, K., Shirayama, M., Trzepacz, C., Brownell, D. R. and Mello, C. C. (2005). Wnt signaling drives WRM-1/beta-catenin asymmetries in early C. elegans embryos. *Genes Dev.* **19**, 1749-1754.
Nance, J. and Zallen, J. A. (2011). Elaborating polarity: PAR proteins and the cytoskeleton. *Development* **138**, 799-809.
Nance, J., Munro, E. M. and Priess, J. R. (2003). C. elegans PAR-3 and PAR-6 are required for apicobasal asymmetries associated with cell adhesion and gastrulation. *Development* **130**, 5339-5350.
O'Brien, L. E., Jou, T. S., Pollack, A. L., Zhang, Q., Hansen, S. H., Yurchenco, P. and Mostov, K. E. (2001). Rac1 orientates epithelial apical polarity through effects on basolateral laminin assembly. *Nat. Cell Biol.* **3**, 831-838.
Piekny, A. J., Johnson, J. L., Cham, G. D. and Mains, P. E. (2003). The Caenorhabditis elegans nonmuscle myosin genes nmy-1 and nmy-2 function as redundant components of the let-502/Rho-binding kinase and mel-11/myosin phosphatase pathway during embryonic morphogenesis. *Development* **130**, 5695-5704.
Portereiko, M. F. and Mango, S. E. (2001). Early morphogenesis of the Caenorhabditis elegans pharynx. *Dev. Biol.* **233**, 482-494.
Priess, J. R., Schnabel, H. and Schnabel, R. (1987). The glp-1 locus and cellular interactions in early C. elegans embryos. *Cell* **51**, 601-611.
Pruss, R. M., Mirsky, R., Raff, M. C., Thorpe, R., Dowding, A. J. and Anderton, B. H. (1981). All classes of intermediate filaments share a common antigenic determinant defined by a monoclonal antibody. *Cell* **27**, 419-428.
Raharjo, W. H., Ghai, V., Dineen, A., Bastiani, M. and Gaudet, J. (2011). Cell architecture: surrounding muscle cells shape gland cell morphology in the Caenorhabditis elegans pharynx. *Genetics* **189**, 885-897.
Rasmussen, J., English, K., Tenlen, J. and Priess, J. (2008). Notch signaling and morphogenesis of single-cell tubes in the C. elegans digestive tract. *Dev. Cell* **14**, 559-569.
Rocheleau, C. E., Yasuda, J., Shin, T. H., Lin, R., Sawa, H., Okano, H., Priess, J. R., Davis, R. J. and Mello, C. C. (1999). WRM-1 activates the LIT-1 protein kinase to transduce anterior/posterior polarity signals in C. elegans. *Cell* **97**, 717-726.
Ryan, M. C., Lee, K., Miyashita, Y. and Carter, W. G. (1999). Targeted disruption of the LAMA3 gene in mice reveals abnormalities in survival and late stage differentiation of epithelial cells. *J. Cell Biol.* **145**, 1309-1323.
Santella, A., Du, Z., Nowotschin, S., Hadjantonakis, A. K. and Bao, Z. (2010). A hybrid blob-slice model for accurate and efficient detection of fluorescence labeled nuclei in 3D. *BMC Bioinformatics* **11**, 580.
Sawyer, J. M., Harrell, J. R., Shemer, G., Sullivan-Brown, J., Roh-Johnson, M. and Goldstein, B. (2010). Apical constriction: a cell shape change that can drive morphogenesis. *Dev. Biol.* **341**, 5-19.
Schonegg, S., Constantinescu, A. T., Hoege, C. and Hyman, A. A. (2007). The Rho GTPase-activating proteins RGA-3 and RGA-4 are required to set the initial size of PAR domains in Caenorhabditis elegans one-cell embryos. *Proc. Natl. Acad. Sci. USA* **104**, 14976-14981.
Smyth, N., Vatansever, H. S., Murray, P., Meyer, M., Frie, C., Paulsson, M. and Edgar, D. (1999). Absence of basement membranes after targeting the LAMC1 gene results in embryonic lethality due to failure of endoderm differentiation. *J. Cell Biol.* **144**, 151-160.
Sulston, J. E., Schierenberg, E., White, J. G. and Thomson, J. N. (1983). The embryonic cell lineage of the nematode Caenorhabditis elegans. *Dev. Biol.* **100**, 64-119.
Tenlen, J. R., Schisa, J. A., Diede, S. J. and Page, B. D. (2006). Reduced dosage of pos-1 suppresses Mex mutants and reveals complex interactions among CCCH zinc-finger proteins during Caenorhabditis elegans embryogenesis. *Genetics* **174**, 1933-1945.
Totong, R., Achilleos, A. and Nance, J. (2007). PAR-6 is required for junction formation but not apicobasal polarization in C. elegans embryonic epithelial cells. *Development* **134**, 1259-1268.
Urbano, J. M., Torgler, C. N., Molnar, C., Tepass, U., López-Varea, A., Brown, N. H., de Celis, J. F. and Martín-Bermudo, M. D. (2009). Drosophila laminins act as key regulators of basement membrane assembly and morphogenesis. *Development* **136**, 4165-4176.
Wallenfang, M. R. and Seydoux, G. (2000). Polarization of the anterior-posterior axis of C. elegans is a microtubule-directed process. *Nature* **408**, 89-92.
Wang, A. Z., Ojakian, G. K. and Nelson, W. J. (1990). Steps in the morphogenesis of a polarized epithelium. I. Uncoupling the roles of cell-cell and cell-substratum contact in establishing plasma membrane polarity in multicellular epithelial (MDCK) cysts. *J. Cell Sci.* **95**, 137-151.
Williams, B. D. and Waterston, R. H. (1994). Genes critical for muscle development and function in Caenorhabditis elegans identified through lethal mutations. *J. Cell Biol.* **124**, 475-490.
Wong, L. L. and Adler, P. N. (1993). Tissue polarity genes of Drosophila regulate the subcellular location for prehair initiation in pupal wing cells. *J. Cell Biol.* **123**, 209-221.
Yochem, J., Gu, T. and Han, M. (1998). A new marker for mosaic analysis in Caenorhabditis elegans indicates a fusion between hyp6 and hyp7, two major components of the hypodermis. *Genetics* **149**, 1323-1334.
Yurchenco, P. D. (2011). Basement membranes: cell scaffoldings and signaling platforms. *Cold Spring Harb. Perspect. Biol.* **3**, a004911.
Zhong, M., Niu, W., Lu, Z. J., Sarov, M., Murray, J. I., Janette, J., Raha, D., Sheaffer, K. L., Lam, H. Y., Preston, E. et al. (2010). Genome-wide identification of binding sites defines distinct functions for Caenorhabditis elegans PHA-4/FOXA in development and environmental response. *PLoS Genet.* **6**, e1000848.
Zhu, X., Joh, K., Hedgecock, E. M. and Hori, K. (1999). Identification of epi-1 locus as a laminin alpha chain gene in the nematode Caenorhabditis elegans and characterization of epi-1 mutant alleles. *DNA Seq.* **10**, 207-217.
Ziel, J., Hagedorn, E., Audhya, A. and Sherwood, D. (2009). UNC-6 (netrin) orients the invasive membrane of the anchor cell in C. elegans. *Nat. Cell Biol.* **11**, 183-189.